Apoptosis (2013) 18:347–360
DOI 10.1007/s10495-012-0794-2

ORIGINAL PAPER

Targeting Chk2 improves gastric cancer chemotherapy by impairing DNA damage repair

A. Gutiérrez-González · C. Belda-Iniesta · J. Bargiela-Iparraguirre · G. Dominguez · P. García Alfonso · R. Perona · I. Sanchez-Perez

Published online: 28 December 2012

Abstract Our results demonstrate that the addition of cisplatin after paclitaxel-induced mitotic arrest was more effective than individual treatment on gastric adenocarcinoma cells (MKN45). However, the treatment did not induce benefits in cells derived from lymph node metastasis (ST2957). Time-lapse microscopy revealed that cell death was caused by mitotic catastrophe and apoptosis induction, as the use of the caspase inhibitor z-VAD-fmk decreased cell death. We propose that the molecular mechanism mediating this cell fate is a slippage suffered by these cells, given that our Western blot (WB) analysis revealed premature cyclin B degradation. This resulted in the cell exiting from mitosis without undergoing DNA damage repair, as demonstrated by the strong phosphorylation of H2AX. A comet assay indicated that DNA repair was impaired, and Western blotting showed that the Chk2 protein was degraded after sequential treatment (paclitaxel-cisplatin). Based on these results, the modulation of cell death during mitosis may be an effective strategy for gastric cancer therapy.

Keywords Cancer · Mitosis · Cisplatin · DNA damage response

A. Gutiérrez-González · J. Bargiela-Iparraguirre · I. Sanchez-Perez
Department of Biochemistry, School of Medicine, UAM, Madrid, Spain

A. Gutiérrez-González · J. Bargiela-Iparraguirre · R. Perona · I. Sanchez-Perez (✉)
Biomedical Research Institute of Madrid, Madrid CSIC/UAM, C/Arturo Duperier 4, 28029 Madrid, Spain
e-mail: misanchez@iib.uam.es

C. Belda-Iniesta
Thoracic, Head & Neck and Brain Oncology Unit, CIOCC Centro integral Oncológico Clara Campal. GHM Grupo Hospital de Madrid, Madrid, Spain

C. Belda-Iniesta · R. Perona
Biomarkers and Experimental Therapeutics Group, IdiPAZ, University Hospital La Paz, Madrid, Spain

G. Dominguez
Department of Medical Oncology, University Hospital Puerta de Hierro, UAM, Madrid, Spain

P. García Alfonso
Department of Medical Oncology, Gregorio Marañon Hospital, Madrid, Spain

R. Perona
CIBER on Rare Diseases (CIBERER), Valencia, Spain

Abbreviations

CDDP	Cisplatin
PXL	Paclitaxel
SAC	Spindle assembly checkpoint
DDR	DNA damage response
DSBs	Double strand breaks
ATM	Ataxia-telangiectasia mutated
ATR	ATM- and Rad3-related
γH2AX	Phosphorylated H2AX
CIN	Chromosome instability
BRCA1	Breast cancer 1

Introduction

Gastric cancer (GC) remains one of the leading causes of cancer mortality worldwide, although its incidence has been decreasing in recent years. Recent epidemiologic studies estimate that approximately 0.9 million cases of GC

are diagnosed annually worldwide. In more than half of all cases, the disease has advanced by the time of diagnosis. Despite potentially curative resection, only 45 % of patients will be free of disease at 5 years [1]. Systemic chemotherapy is therefore essential for the management of advanced GC because it improves survival and quality of life; however, there is no standard patient regimen. Several chemotherapeutic regimens have been established as first-line therapies, and they have contributed to improved survival [2]. After this first therapeutic intervention, 30–70 % of patients receive second-line chemotherapy. Among the various regimens, paclitaxel (PTX) or docetaxel combined with fluorouracil plus cisplatin (PCF), oxaliplatin combined with fluorouracil plus leucovorin (FOLFOX-4) or with capecitabine and epirubicin [3] are the most commonly used therapies [4, 5]. Furthermore, there are patients whose tumors overexpress the epidermal growth factor receptor isotype 2 (Her-2/neu/c-Erb-2) [6, 7]. In these cases, employing a platinum doublet and replacing epirubicin or docetaxel with an antibody directed against the extracellular domain of the transmembrane protein has led to an overall increase in survival of over 30 % in a recent clinical trial [8, 9]. Unfortunately, given that none of these treatments have proven ideal in terms of overall survival, schedule selection is based on patient performance, previous experience with a particular drug combination and potential toxicity studies [10]. The taxanes, paclitaxel and docetaxel, are microtubule-stabilizing agents that induce cell-cycle arrest at the G2/M stage. Both agents have been used to treat advanced gastric cancer. Several clinical trials have shown an improvement in response to drug combinations, using paclitaxel or docetaxel for first-line and cisplatin and 5-FU for second-line treatments [11]. However, the reasons for the positive effects at the molecular level of such combinations are not known, nor is it known which new drugs against given therapeutic targets would further improve the course of the disease.

DNA damage inflicted by genotoxic drugs triggers the DNA damage response (DDR) pathway [12], [13]. The DDR involves a complex network of proteins that cooperate to initiate and coordinate cell-cycle progression, DNA repair and cell death. Two major phosphatidylinositol-3 (PIK)-like proteins, ATM and ATR, act in response to DNA damage. Once activated, these proteins activate the transducer proteins Chk1, Chk2, p53 and BRCA1, among others [14, 15]. Chk1 and Chk2 can phosphorylate several key substrates, such as the Cdc25 family [16–18], leading to G2 phase arrest, which protects cells from entering mitosis in the presence of DNA damage [19]. The decision by the cell to enter mitosis is mediated by a network of proteins that regulate activation of the cyclin B–Cdk1 complex. Cyclin B levels are periodically regulated by transcription and degradation cycles. Thus, Cdk1 must be phosphorylated on its T loop for full activity, and Cdk1 T14 and Y15 phosphorylation is controlled by the balance between Wee1/Myt1 kinases and Cdc25 phosphatases. In human cells, high cyclin B levels are temporally restricted to the G2 phase and early mitosis by regulated transcription and protein degradation. Degradation of cyclin B is regulated by the anaphase-promoting complex/cyclosome (APC/C), a multisubunit E3 ligase that can polyubiquitinate numerous mitotic regulators, and is therefore targeted for destruction by the proteasome. Polyubiquitination of cyclin B starts in the metaphase, when the spindle assembly checkpoint (SAC) is silenced [20]. In addition to direct regulation of Cdk1 T14/Y15 phosphorylation, several feedback mechanisms regulate cyclin B–Cdk1 activation indirectly, such as PlKs and Aurora protein kinases [21].

A number of studies have reported that after prolonged treatment with microtubule-targeted drugs, cells overcome the mitotic delay in a process termed mitotic slippage, adaptation or leakage [22]. The degradation of cyclin B has been shown to play an important role in mitotic slippage, although the details of the molecular mechanisms are not fully understood. Generally, cells treated with microtubule-binding drugs undergo mitotic catastrophe due to mitotic slippage. Mitotic catastrophe is characterized by the appearance of enlarged micronucleated or multinucleated cells [23]. The eventual fate of cells suffering from mitotic catastrophe is usually apoptosis. Mcl-1 is a pro-survival member of the Bcl-2 protein family, and its function is to suppress apoptosis during mitosis. However, under an apoptotic stimulus, this protein is phosphorylated by JNK, p38 and CKII, which promotes degradation by the proteasome and, as a consequence, induces cell death [24]. Cells exposed to genotoxic agents are arrested at different phases of the cell cycle by activation of G1, S or G2/M checkpoints in order to provide sufficient time for DNA repair. In mammalian cells, homologous recombination (HR) and non-homologous end joining (NHEJ) are the two main pathways involved in the repair of DNA double-strand breaks [25]. BRCA proteins act in the DNA repair pathway that involves homologous recombination (HR) and are essential for the repair of double-strand breaks [26].

Previously, we demonstrated that nocodazole sensitizes cisplatin-induced apoptosis in colon carcinoma cells. We showed that these cells suffer from chromosome instability (CIN) due to increased levels of SAC proteins and defects in the DNA damage response [27]. In this study, we used a specific strategy for sensitizing GC cells to cisplatin, which consists of sequential treatment with paclitaxel followed by cisplatin. To gain insight into the molecular parameters that determine cell fate after the mitotic arrest induced by this treatment strategy, we analyzed the mechanisms triggering cell death in tumor cell lines that respond differently to

cisplatin. First, we demonstrated that adenocarcinoma MKN45 cells die due to mitotic catastrophe once they become trapped in mitosis. In contrast, lymph-node metastatic ST2957 cells remained arrested in mitosis. We proposed that MKN45 cells escaped from mitosis, a fact attributable to the inactivation of the cyclin B-Cdk1 complex, and eventually died by apoptosis. Furthermore, we found that Chk2 activity was impaired in response to the treatment, and as a consequence, BRCA1-mediated DNA repair decreases.

Materials and methods

Reagents

Cisplatin, paclitaxel and ChkII were purchased from Sigma Aldrich CO LLC, Spain. z-VAD-fmk was purchased from Vitro S.A., Madrid, Spain.

Cell culture

The MKN45 (poorly differentiated adenocarcinoma) (DSMZ: Deutsche Sammlung von Mikroorganismen und Zellkulturen GmbH) cell line was maintained in RPMI 1640 supplemented with 10 % FBS and 2 mM L-Glutamine. ST2957 cells (lymph node metastases) [28] (ATCC/LGC Standards, Spain) were maintained in high glucose Dulbecco's Modified Eagle Medium (DMEM; Gibco), supplemented with 2 mM L-Glutamine, 1 mM sodium pyruvate and 10 % fetal bovine serum. All cell lines were grown at 37 °C in a humidified atmosphere containing 5 % CO_2.

Cell viability assays

Viability was determined using a crystal violet-based staining method, as described previously [29]. Briefly, 5×10^4 cells per well were seeded in 24 multiwell dishes, treated with various amounts of the selected agent for 24 h and fixed with 1 % glutaraldehyde. After they were washed in 1X PBS, cells were stained with 0.1 % crystal violet. A colorimetric assay using 595 nm Elisa was used to estimate the number of cells per well.

Cell cycle analysis

After appropriate treatment, adherent and non-adherent cells were harvested and fixed overnight in 70 % ethanol in phosphate-buffered saline (PBS). For DNA content analysis, the cells were centrifuged and resuspended in PBS containing 1 μg/ml RNase (Qiagen Ltd., Crawley, UK) and 25 μg/ml propidium iodide, incubated at room temperature for 30 min, and finally analyzed using a Becton–Dickinson Flow Cytometer (Cowley, UK). Data were plotted using Cell Quest software, with 10,000 events analyzed per sample.

Western blotting

Protein extracts (20 μg) were resolved on 4–20 % SDS-PAGE (BioRad) and transferred to nitrocellulose membranes. An immunoblot analysis was performed as described previously [27]. The following antibodies were used in the experiments: cyclin B (Santa Cruz), Chk2 (A-12, Santa Cruz), $Chk2^{Ser19}$, $Chk2^{thr68}$, Histone $H3^{Ser10}$, p-P38, (Cell Signaling, Charlottesville, USA), BRCA1 (Santa Cruz Biotechnology, Inc. Germany), $p53^{Ser15}$, p53, H2A-X^{Ser139} (Upstate), $CDC25C^{Ser216}$, α-Tubulin (Sigma-Aldrich, USA), ATM-^{S1081P} (Rockland Immunochemicals) ATM (Novus Biologicals), Mcl-1 (Santa Cruz Biotechnology Inc., Germany) p-JNK (Promega Corporation, Spain), and secondary antibodies conjugated to horseradish peroxidase (Biorad, Spain). Blots were developed using enhanced chemiluminescence detection system (ECL Santa Cruz Biotechnology, USA).

Immunofluorescence

Cells were fixed and fluorescence microscopy was performed using a NIKON Eclipse 90i. Image analysis was performed with the Nikon NIS-Elements software program and processed using Image J. For high-throughput microscopy, cells were grown on micro-clear-bottom 96-well dishes (Greiner Bio One) and analyzed with a bioimager (Pathway 855; BD). Image acquisition (ORCA 1394; Hamamatsu Photonics) was performed at room temperature using oil as an immersion media and a 40 × 0.75 NA Plan Apo objective (HCX). Image analysis was performed with imaging software (Altovision; BD). All images for quantitative analyses were acquired under nonsaturating exposure conditions. Primary antibodies included γ-H2AX^{Ser139} (Millipore). Secondary antibodies were conjugated with Alexa Fluor 488 (Invitrogen). DAPI (Invitrogen) was used for DNA staining.

Time-lapse microscopy

For live-cell analyses, MKN45 cells were grown in an Ibidi μ-Slide 8-well chamber (IBIDI LLC Martinsried, Germany) transfected with Lipofectamine 2000 (Invitrogen) with 0.5 μg of pBOS-H4B-GFP per well (a gift from Dr. M. Malumbres) followed by time-lapse microscopy using the Cell Observer Z1 (Zeiss) at 37 °C and 5 % CO_2/95 % air, AxioVision 4.8 imaging software and a Cascade 1 k camera. Images were taken every 10 min and further

processed using AxioVision digital image processing software (Zeiss). Cells were filmed during a 24-h period, and every 10 min a bright field and a fluorescent image were captured.

Comet assay

We performed the comet assay under alkaline conditions as described by Singh et al. [30]. CDDP was added at a concentration of 10 μg/mL for 4 h. Cells exposed to the sequential treatment were preincubated for 24 h with paclitaxel and then treated for 4 h with CDDP. For the repair assay, cells were allowed to recover from the induced damage by washing in PBS and incubating at 37 °C with fresh media for 1, 2.5 and 4 h before harvesting. Experiments were performed in duplicate. Fifty comets per duplicate gel were scored and quantified by Komet 5.5 image analysis software (Kinetic Imaging Ltd., Nottingham, UK). Apoptotic cells (nondetectable cell nuclei, ghost cells, clouds or hedgehogs) were not scored.

shRNA lentiviral particle transduction

Chk2 shRNA (h) and control shRNA lentiviral particles were purchased from Santa Cruz Biotechnology, Inc. Transduction was performed according to the manufacturer's instructions. Briefly, cells were seeded in 12 multiwell dishes, and infection was performed in the presence of polybrene (5 ug/ml) overnight. For the selection of stable clones, cells were split and cultured in growth medium containing puromycin 3 μg/ml. Resistant clones were expanded and assayed for stable shRNA expression. Reductions in gene expression were analyzed by quantitative/real-time PCR (QPCR) and compared to non-silencing shRNA. Protein levels were analyzed by immunoblot.

cDNA preparation and QPCR

Total cellular RNA was extracted using Tri-Reagent (Life Technologies, Carlsbad, CA, USA) according to the manufacturer's instructions, and reverse transcription was performed on 2 μg of total RNA using M-MLV reverse transcriptase (Promega, Madison, WI, USA). The primer sets used to amplify specific sequences were 5′- ATCCA AAGGCACGTTTTACG-3′ and 5′- ACAACACAGCAGC ACACACA-3′ for Chk2; and 5′-GAT GGT ACA TGA CAA GGT GC-3′ for GADPH. The quantitative expression of each gene was measured by SYBR Green polymerase chain reaction assay. Statistical analyses were performed for each gene by using a paired t test to compare mean values. Values of $p < 0.05$ were considered significant. Relative quantification (RQ) was achieved using the delta-Ct method in which each 1-Ct difference equals a 2-fold change in transcript abundance.

Statistical analysis

Statistical significance was analyzed using a two-tailed Student's t test; * $p < 0.05$; ** $p < 0.005$.

Results

Paclitaxel sensitizes GC cells to cisplatin by mitotic catastrophe and apoptosis induction

First, we assayed combination modalities of cisplatin (CDDP) with paclitaxel (PXL) in various GC cell lines to assess which treatment was more effective. We studied the viability of MKN45 (poorly differentiated GC cells) and ST2957 (lymph node metastases) adenocarcinoma GC cell lines after exposure to two modalities of treatment. We treated both cell lines either with serial concentrations of CDDP (0–20 μg/ml) or sequentially by pretreating cells with 0.1 μM PXL for 20 h and, after PXL removal, treating them with CDDP as above (PXL-CDDP). We found a modest but statistically significant toxic effect in MKN45 cells after sequential treatment with PXL and CDDP; however, this combination did not have as deleterious an effect on ST2957 cells after 24 h of treatment (Fig. 1a). In order to visualize cell death, we performed immunofluorescence studies with DAPI staining after treatment of GC cells with the various drug combinations. We observed that CDDP and PXL-CDDP led to an accumulation of cells displaying morphological changes characteristic of apoptosis or mitotic catastrophe (MC), such as the formation of apoptotic bodies, chromosome dispersion and micronucleation at 24 h (Fig. 1b). After quantification of the cells showing these morphological features, we found a steep increase in MKN45 cells showing signs of death when compared with ST2957 cells (21 vs 7 %) 24 h after the sequential treatment. In mitotic catastrophe, a cell is destroyed during mitosis or after a faulty mitosis. To follow the behavior of individual cells, we transiently transfected MKN45 cells with GFP-tagged histone H4B (Fig. 1c) and studied the duration of the mitosis. We recorded this information by measuring the duration of the interval between the exact moment when a cell enters mitosis (the interphase-prophase transition or IPT) and the moment when it exits mitosis (the metaphase-anaphase transition or MAT) using time-lapse microscopy. These transition points were chosen because they represent the two key steps in mitotic progression that are regulated by the cell cycle machinery. We showed that the mitotic duration for MKN45-untreated cells is 70 min on average. After

cisplatin treatment the mitotic duration was 90 min. In contrast, paclitaxel, which prolongs mitosis by activating the spindle checkpoint, induced a delay in mitosis up to an average of 120 min. However, sequential treatment with PXL followed by CDDP increased the duration of mitosis to nearly 200 min. We also studied the cells' fate after these treatments and detected that a number of the mitosis processes were accompanied by mitotic catastrophe 4–6 h after the treatments, and overall cell death increased by up to 50 % (Fig. 1d). Collectively, our findings suggest that the PXL-mediated mitotic arrest might have contributed to an increased sensitivity to the proapoptotic actions of CDDP in MKN45 cells.

MKN45 cells suffering from mitotic catastrophe die via apoptosis

To better define the mechanisms of action of PXL-CDDP treatment in inducing MC and/or apoptosis, DNA flow cytometry analysis was performed to determine whether cell cycle perturbations could be responsible for the increase in cytotoxicity induced by the treatment (Fig. 2a). Treatment of MKN45 and ST2957 cells with PXL for 20 h induced an accumulation of cells in the G2/M phase of the cell cycle (around 84 %), but 24 h after PXL removal, the G2/M cell content decreased to 50 %, and the number of apoptotic cells increased (18 %) in MKN45 cells. In contrast, ST2957 cells remained in G2/M (70 %) 24 h after PXL removal. Cisplatin treatment induced apoptosis both in MKN45 (28 %) and ST2957 (9 %) cells. Nevertheless, after PXL-CDDP exposure, only MKN45 cells showed an increase in the percentage of apoptosis (50 %), concomitantly with an important reduction in G2/M cell content (19 %). Although an increase in apoptosis was also observed in ST2957 cells after PXL-CDDP treatment, this effect was not additive, at least at 24 h after treatment, as the majority of cells remained in the G2/M phase (Fig. 2a). Taking into account that these cell lines have chromosomal instability, we did not observe a significant change in aneuploidy population after treatment. Caspase activation is a predictor of cell death and a clear feature of apoptosis. Western blot analysis was used to confirm apoptosis as a mechanism of cell death by analyzing caspase activation through the harvesting of asynchronous cell cultures after treatment with CDDP or PXL-CDDP over a time period of 1–24 h. We studied the activation of caspase-3 by immunoblotting with an antibody against cleaved PARP (a substrate of caspase-3) and observed that CDDP strongly induced PARP's cleavage 24 h after treatment in MKN45 cells, while in PXL/CDDP-treated cells, the cleavage was detected earlier, at only 9 h after drug exposure. In contrast, in ST2957 cells, the kinetics of PARP cleavage were the same regardless of the treatment, and cleavage was almost undetectable in these cells (Fig. 2b, left panel). Accordingly, caspase-3 was strongly activated in MKN45 cells treated with PXL-CDDP (3 h) (Fig. 2b, right panel) and was barely detected, at least at this time, in ST2957 cells (not shown). Mcl-1 is a pro-survival member of Bcl-2 protein family, and its function is to suppress apoptosis during mitosis. However, under apoptotic stimulus this protein is phosphorylated by JNK, p38 and CKII, promoting degradation by the proteasome and, as a consequence, the induction of cell death. The results we present above encouraged us to study the status of Mcl1 in cells treated with PXL-CDDP, where we observed a strong activation of JNK and p38 stress kinases either after CDDP or PXL-CDDP, with the same kinetics for both (Fig. 2c). However, Mcl-1′s small fragment was detected only in MKN45 cells, indicating that the mechanism of apoptotic induction is activated in these cells after PXL-CDDP treatment (Fig. 2c). The additive effect observed in apoptosis induction for PXL-CDDP was abolished by the pan-caspase inhibitor z-VAD-fmk (Fig. 2d). The inhibition of apoptosis correlated with a net increase in the number of cells that accumulated into the G2/M phase of the cell cycle, strongly suggesting that cell death occurred during the mitotic phase of the cell cycle.

Cisplatin-induced mitotic catastrophe is due to mitotic slippage after a prolonged mitotic arrest in MKN45 cells

The results of the flow cytometry analysis did not clearly elucidate the characteristics of the cell cycle arrest in G2/M or mitosis. To determine whether the MKN45 cells were arrested specifically in mitosis or G2 before dying and after PXL-CDDP treatment, we examined the molecular status of the G2/M checkpoint by analyzing the expression of cell-cycle regulatory proteins. Mitotic histone H3 phosphorylation occurs at Ser10, and there is a close correlation between H3 phosphorylation, chromosome condensation and segregation during mitosis. Consistent with these phenomena, $H3^{Ser10}$ phosphorylation, a marker of mitosis, was stimulated (after PXL-CDDP treatment) for approximately 6 h in MKN45 cells and for 9 h in ST2957 cells (Fig. 3a). Next, we analyzed the expression of the cell cycle-related proteins Cdc2, Cdc25c and cyclin B1 that control G2/M transition. Phosphorylated $CDC25C^{Ser216}$ and $Cdc2^{Tyr15}$ downregulate the activation of the cyclin B1-cdc2 complex. Our Western blot analysis showed that PXL induced an increase in Ser216 and Tyr15 inhibitory phosphorylation both on Cdc25C and Cdc2, which was maintained for 6 and 9 h after CDDP exposure in MKN45 and ST2957 cells, respectively, indicating the activation of the G2 checkpoint (Fig. 3b). Another mechanism regulating Cdc2 activity and thus progression into the mitotic

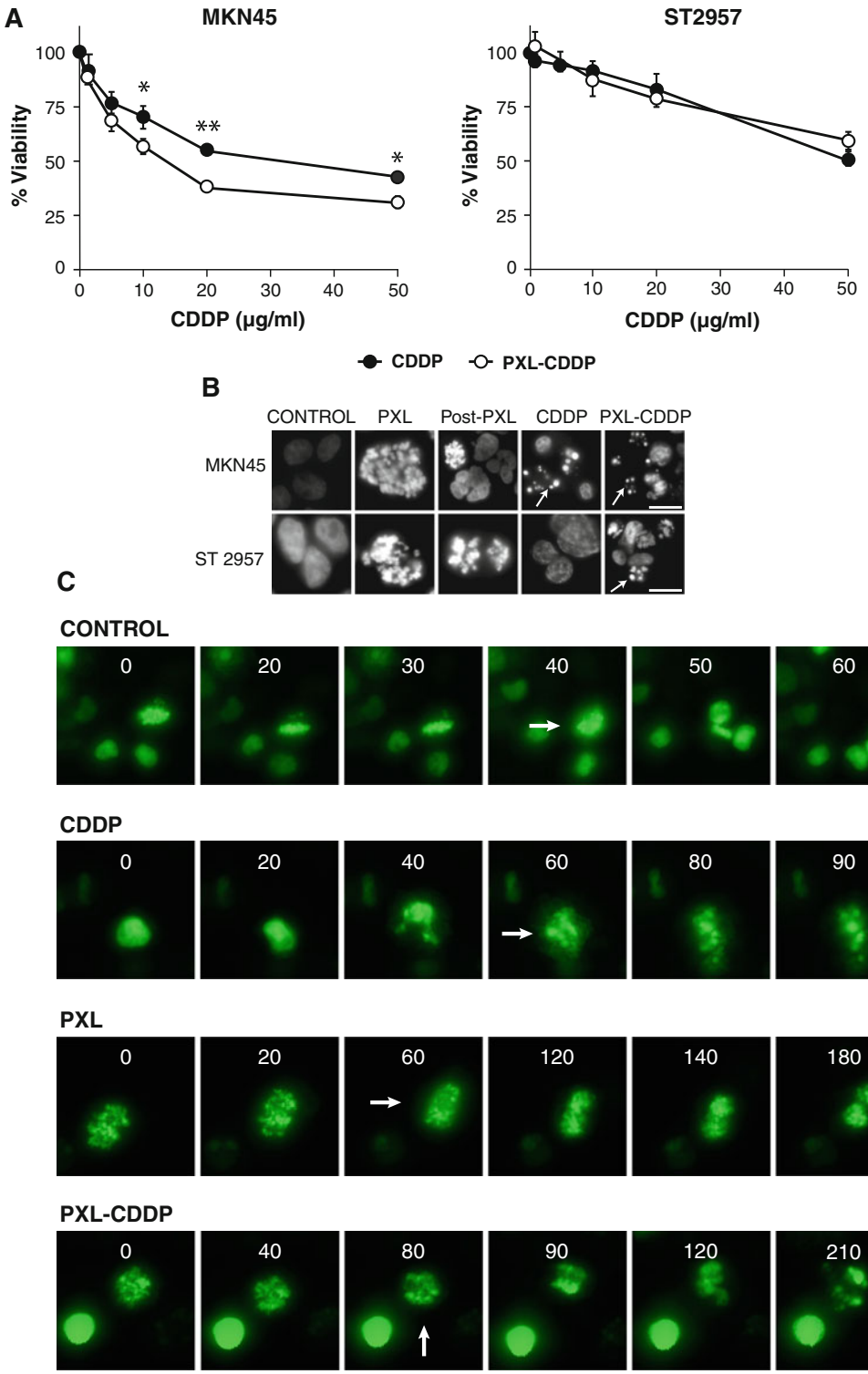

D

	MD (n=20 Movies)	% Cell Death
Control	70 ± 12	3
CDDP	90 ± 10	7
PXL	120 ± 15	20
PXL-CDDP	200 ± 20	53

◀ **Fig. 1** Survival of MKN45 and ST2957 cells after treatment with CDDP or sequential treatment with PXL and CDDP. **a** MKN45 and ST2957 cell lines were treated with increasing amounts of CDDP (0–50 μg/ml) (*filled circles*), or pretreated with PXL (0.1 μM) overnight and then washed and exposed to CDDP (*open circles*). Viability was quantified using the crystal violet method 24 h after treatment. The percentage is shown as relative to the number of cells without treatment. Data represent the means of two experiments performed in quadruplicate. Statistical analysis was performed using Student's *t* test (* $p < 0.05$; ** $p < 0.005$). **b** Cells were treated with CDDP (15 μg/ml), PXL (0.1 μM), PXL-CDDP (0.1 μM–15 μg/ml) for 24 h. Then, cells were fixed with PFA 3.7 % and stained with DAPI. *Arrows* show cell death with fragmented DNA. *Scale bar* 10 μ C. MKN45 cells were transiently transfected with 0.5 μg of pBOS-H4-GFP. 24 h after transfection cells were untreated or treated with CDDP (10 μg/ml); PXL (0.1 μM) overnight, then washed and changed to either fresh medium alone (PXL) or fresh medium plus CDDP (PXL-CDDP). The progression through mitosis of cells expressing GFP-tagged histone H4B was monitored by live-cell microscopy, and typical examples of image sequences are given. *Scale bar* 20 μ. The *graph bar* represents $n = 20$ movies. Table shows the quantification of the mitotic duration (MD) in the studied conditions ($n = 20$ movies) and percentage of cell death in the cells after the various treatments, $n = 100$ cells

phase is the complex formation with cyclin-B1. We then determined endogenous levels of cyclin-B1 and detected an accumulation of this protein after PXL-CDDP treatment in both cell lines. However, in MKN45 cells, a slow and continuous decrease still took place, probably due to the incomplete inhibition of the APC/C, unlike ST2957 cells, which only showed a decrease at 24 h. Together, the data suggests that mitotic slippage in MKN45 cells might be due to the inactivation of the cyclin B1-cdc2 complex after treatment with PXL and then CDDP. This result suggests an exit from mitosis before the cells manage to repair the damage induced by the drugs.

Paclitaxel potentiated cisplatin-induced activation of the DNA damage response (DDR)

To directly assess the consequences of PXL pretreatment in the cellular response to DNA damage, we first analyzed the levels of $\gamma H2AX^{Ser139}$ as a marker of DSBs after cisplatin challenge using high-throughput imaging (HTI) analysis. 6 hours after cisplatin addition, a significant increase in γH2AX foci was observed in PXL-pretreated MKN45 cells, suggesting that these cells are able to detect the CDDP-induced DSBs that remain unrepaired before they enter mitosis, which is in agreement with our in vivo analysis (Fig. 4a, left panel). To further evaluate this result, we studied the kinetics of γH2AX phosphorylation by Western blot comparing asynchronous cell cultures with mitotic cells after cisplatin treatment. In MKN45 cells, DNA damage is detected 9–24 h after treatment with CDDP (Fig. 4a, right panel). However, in PXL-pretreated cells (arrested in the prometaphase), damage is detected earlier (6 h), indicating PXL-potentiated cisplatin induction of DNA damage. Altogether, these findings suggest that MKN45 cells are able to detect DNA damage in mitosis and that this damage is permanent, perhaps because DNA repair was compromised. In contrast, 6 h after the administration of CDDP, ST2957 cells displayed a strong γ-H2AX-signal that declines after PXL/CDDP treatment, suggesting that damage detection by these cells in mitosis may be compromised (Fig. 4a, right panel). Next, we studied other events in the DDR. First, we evaluated the activation of ATM by phosphorylation ($ATM^{Ser1981}$) in GC cells. We did observe CDDP-induced activation of ATM after 3 h of treatment. However, PXL directly activated ATM for at least 24 h. Furthermore, the kinetics of ATM phosphorylation was identical in both cell lines (Fig. 4b). Next, we evaluated the activation of Chk2, and the results showed a significant reduction in both $Chk2^{Thr68}$ and $Chk2^{Ser19}$ phosphorylation levels after PXL-CDDP exposure. The latter was more obvious in MKN45 cells, indicating that this pathway is impaired in this cell line. This impairment may be due to a reduction in Chk2 protein levels, as shown (Fig. 4c). We next analyzed p53 phosphorylation as a measure of ATM activity and found that in both GC cell lines, CDDP treatment induced a drastic increase in $p53^{Ser15}$, in both asynchronous and synchronic cells with similar kinetics (Fig. 4d). Altogether, these results suggest that PXL pretreatment increased chromosomal damage after cisplatin-induced cell death in MKN45 cells, resulting in extensive H2AX phosphorylation and a potentiation of the DDR response in GC cells after cisplatin treatment, which appears to be a direct cause of catastrophic mitosis or apoptosis.

PLX/CDDP treatment induces proteasome-dependent degradation of Chk2

To examine if proteasome activity is involved in the decrease in Chk2 protein levels, we studied whether the proteasome inhibitor MG132 modulated Chk2 protein levels. MKN45 cells showed a reduction in Chk2 in mitotic cells treated with PXL-CDDP, which was inhibited by the addition of MG132 (Fig. 5a). These results prompted us to study whether the application of Chk2 inhibitors improves therapy in GC treatment. In our experience, the selective Chk2 inhibition greatly increased the percentage of apoptosis in GC cells after treatment. In combination with the Chk2 inhibitor (ChkII), cisplatin treatment resulted in approximately a 3-fold increase in apoptosis in MKN45 cells, compared to cisplatin alone. Surprisingly, this effect was not observed in ST2957 cells. However, both cell lines were more sensitive to PXL/CDDP treatment in combination with ChkII (Fig. 5b). These results demonstrate that pharmacological inhibition of the Chk2 pathway may enhance the therapeutic efficacy of platinum compounds in the treatment of GC. To study the contribution of Chk2 in

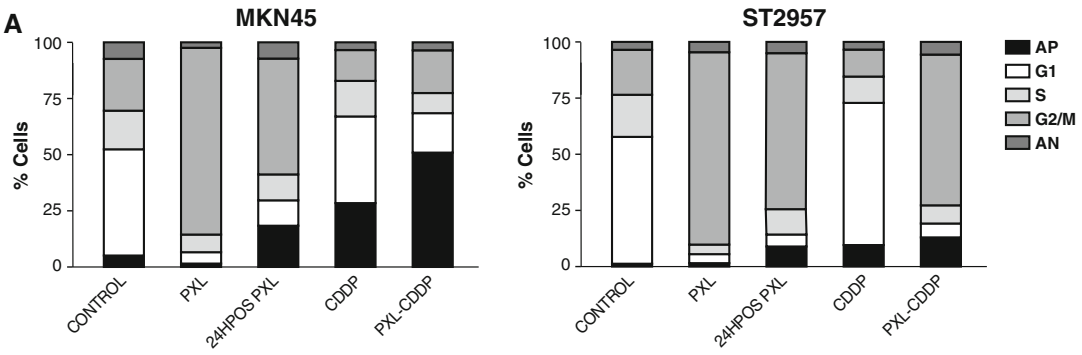

MKN45

	AP	G1	S	G2/M	AN
CONTROL	5.10	47.91	17.43	23.23	6.92
PXL	1.13	5.70	7.61	83.96	1.98
Post-PXL	18.06	12.08	11.52	52.18	6.79
CDDP	28.68	39.26	15.50	14.02	3.00
PXL-CDDP	50.90	18.44	8.51	19.26	2.96

ST2957

	AP	G1	S	G2/M	AN
CONTROL	0.75	57.00	18.48	20.55	3.37
PXL	1.19	4.35	4.17	85.71	4.76
Post-PXL	8.97	5.29	10.53	69.47	5.14
CDDP	9.49	64.44	11.79	12.25	3.35
PXL-CDDP	13.37	6.46	7.56	69.35	5.85

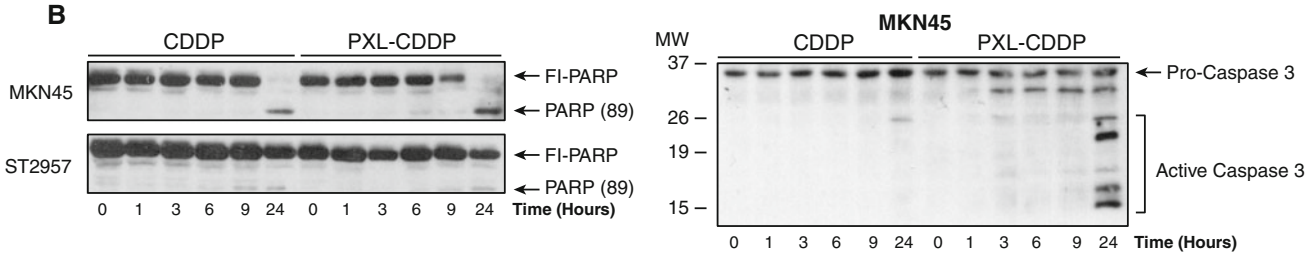

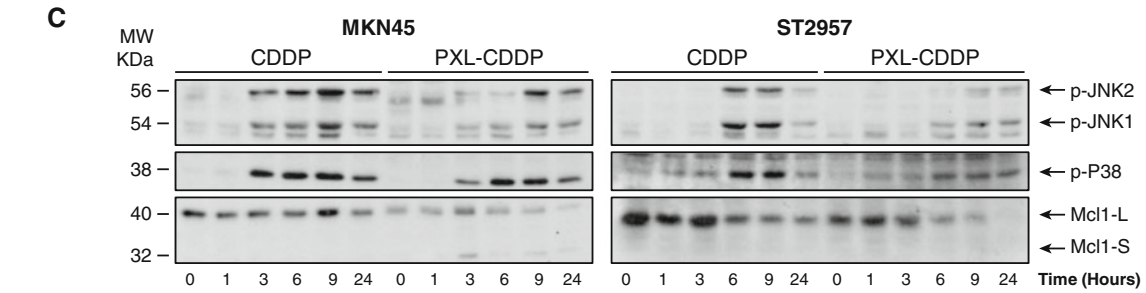

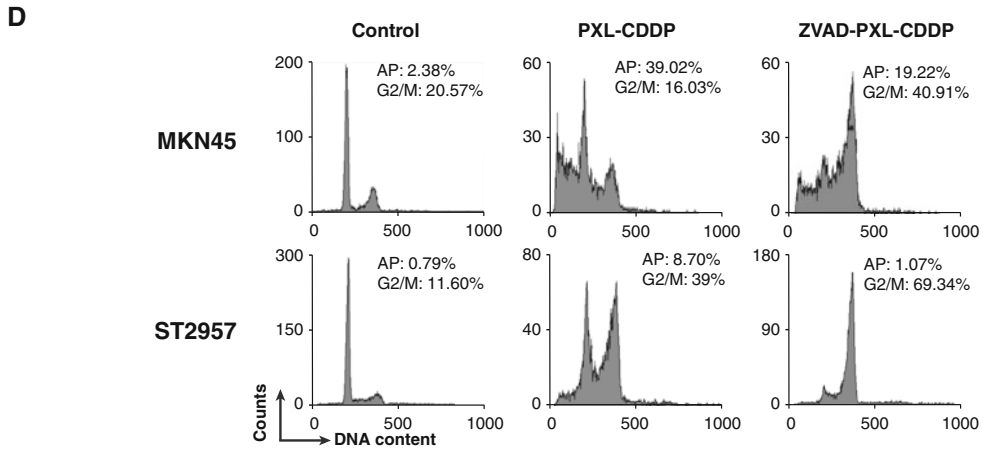

the response to therapy, we abolished Chk2 expression by generating stable cell lines by transduction with Chk2 shRNA (h) lentiviral particles containing a target-specific construct that encodes a 19–25 nt (plus hairpin) shRNA designed to knock down gene expression of Chk2. After selection with puromycin, stable MKN45 cells showed

◀ **Fig. 2** MKN45 cells die during mitosis by mitotic catastrophe and apoptosis induction. **a** Cell cycle analysis of GC cell lines treated with CDDP (10 μg/ml), PXL (0.1 μg/ml) or sequentially treated PXL for 18 h and then treated with CDDP for 24 h. The *graph* represents the percentage of cells in apoptosis (AP), G1, S, G2/M and *aneuploidy >4 N* (AN), indicated in the table below for each cell line in a representative experiment. The experiment was performed three times with similar results. **b** Cells treated with CDDP (10 μg/ml) or cells pretreated with PXL (0.1 μM for 20 h), washed and then treated for 0–24 h with CDDP. Cell lysates were extracted and Western blots were performed using antibodies against PARP and caspase 3. Similar results were obtained in three independent experiments. **c** Mcl-1 is proteolytically processed after sequential treatment in MKN45 cells. Western blots were performed using antibodies against phospho-JNK, phospho-p38 and total Mcl-1 proteins. Similar results were obtained in three independent experiments. **d** Cells were preincubated for 1 h with zVAD-fmk (50 μM) before exposure to the indicated drugs. Cell cycle analyses were performed as in (**a**)

nearly total abolishment of Chk2 mRNA levels and ST2957 showed around 60 % reduction. (Fig. 5c upper graph). This result was confirmed by Western Blot analysis of the cells (Fig 5 lower panel). These cells were used to study the appearance of apoptotic cells after cisplatin treatment. Our results showed that in the absence of Chk2, both cell lines (MKN45 and ST2957) are more hypersensitive to cisplatin, which confirms the pharmacological result. (Fig. 5d).

One of the substrates described for Chk2 during mitosis is BRCA1 [31]. To study the influence of PXL/CDDP treatment on BRCA1-phosphorylation status due to the downregulation of Chk2 during the treatment, we performed Western blot analysis by using a specific antibody against BRCA1. The result showed that both treatments (cisplatin and paclitaxel) individually increased BRCA1 (Ser988) (Fig. 5e, lanes 3 and 4); however, the treatment with PXL/CDDP abolished the phosphorylation of this residue (Fig. 5e, lane 6). To specifically study the contribution of Chk2 to this effect on BRCA1, we used the ChkII inhibitor and observed that the inhibition of Chk2 by ChkII abolished the activation of BRCA1 (Ser988) after CDDP treatment (Fig. 5e, lane 5). These observations suggest that, in the absence of Chk2, the recently identified controller of chromosome segregation, the Chk2-BRCA1 signaling pathway [32, 33], is absent and could increase chromosome instability. The reason for the increased sensitivity of cells to sequential treatment may involve the DNA repair signaling pathway. DNA repair might be impaired in mitosis, and consequently, cytotoxicity may increase after chemotherapy. To investigate whether MKN45 cells were able to repair damage caused by the drugs, we performed a Comet Assay. No differences in either TI or TM were observed in cells where the repair process was not allowed, mainly due to the fact that CDDP-induced adducts are not detected by the Comet Assay. The repair experiments performed at different time points allow the diverse repair systems to detect and excise the induced adducts (these products are now detectable by the Comet Assay). Thus, the values observed in these experiments reflect both the severity of the damage and the repair capability. After 1 h of repair, we observed a higher degree of damage in those cells treated with the sequential treatment than in those treated exclusively with CDDP. These results support the fact that paclitaxel can induce DNA breakage, as has been recently described, thus demonstrating that paclitaxel induces DNA damage due to telomere deprotection during mitotic arrest [34] or to another non-described type of damage [35, 36]. As expected,

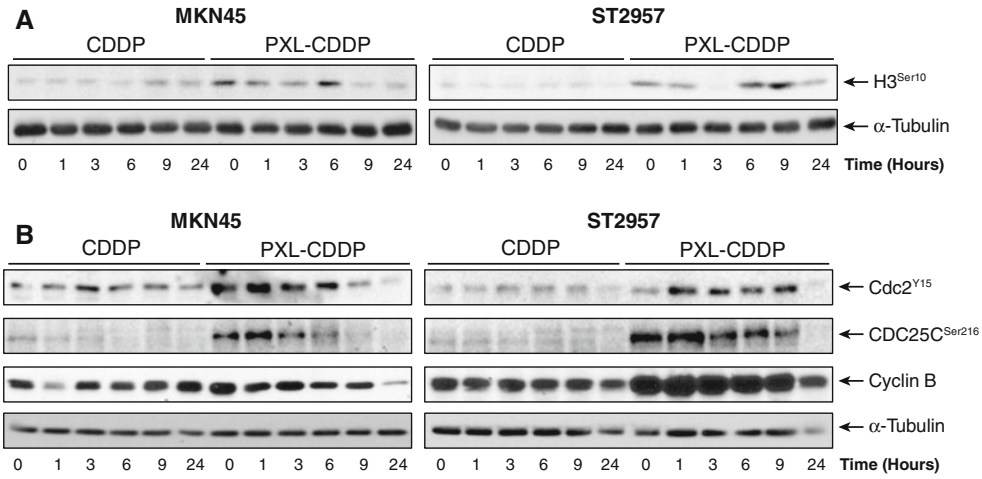

Fig. 3 Cyclin B1 degradation and cdc2 downregulation correlated with mitotic slippage in MKN45 cell after PXL-CDDP treatment. Cells were pretreated or not with PXL (0.1 μM for 20 h), washed and then treated for 0–24 h with 10 μg/ml CDDP. Whole cells extracts were prepared and hybridized with antibodies against **a** HisH3^{ser10,} **b** cdc2^{Y15}, cdc25c^{Ser216} or cyclin-B1. The blots were also probed for α-tubulin to ensure equal protein loading. The experiments were repeated three times with similar results. A representative experiment is shown

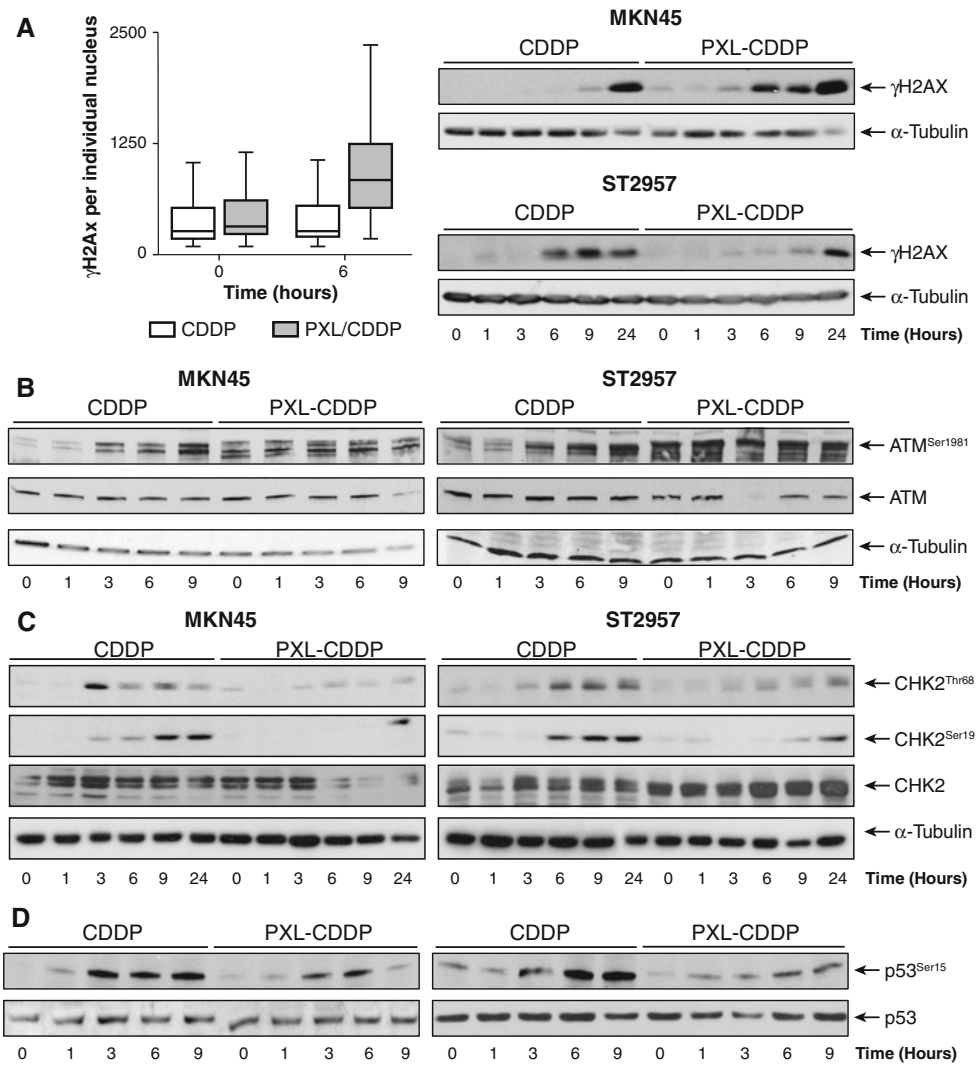

Fig. 4 Paclitaxel potentiated the DNA damage response after Cisplatin treatment in MKN45 cells. **a** Intensity of the γ-H2AX signal per nucleus, measured at the indicated times by high throughput microscopy (HTI). *Each bar* represents the total amount of γ-H2AX found in each nucleus, 6 h after the exposure of MKN45 cells to the treatment. Data are expressed as mean ± SD ($n = 3$). *Right panel*: Extracts from MKN45 and ST2957 cells were harvested at different times after treatment and blotted with antibodies against γ-H2AX. **b** The same extracts from (**a**), blotted with antibodies against $ATM^{Ser1981}$ or ATM. The blots were also probed for α-tubulin to ensure equal protein loading. **c** After treatment with the same schedule, whole cell extracts from MKN45 and ST2957 cells were prepared and blotted against $Chk2^{Ser19}$, $Chk2^{Thr68}$ or Chk2 at the indicated time points. The same extracts from (**a**), blotted with antibodies against $p53^{Ser15}$ and p53. The experiments were repeated three times with similar results. A representative experiment is shown

untreated cells showed the milder degree of damage. As the repair progresses (2.5–4 h), the CDDP-induced damage is almost completely repaired but not the damage induced by the combination of PXL-CDDP, highlighting a deficiency in the repair systems (Fig. 5f). The above results suggest that the increased sensitivity to sequential treatment observed in MKN45 cells is partly due to the inability to induce the homologous repair system mechanism through BRCA1.

Discussion

Despite current advances in the clinical management of GC, there is no therapeutic combination that has proved to be curative for this type of tumor. There have been numerous in vitro studies that predict the prognosis of the disease and studies that reveal molecular targets that, once interfered with, result in increased cell death in response to chemotherapy. However, clinical trials conducted so far, using various combinations of drugs, have not shown an improvement in the management of the disease. The experiments presented here direct us to a novel observation: eliminating cells during mitosis may be an ideal strategy for sensitizing gastric cells to therapy. However, the selected target depends on the subtype of cancer; therefore, understanding the various mechanisms of action of the drugs and discovering new therapeutic targets is crucial to using this strategy successfully. We have demonstrated that gastric adenocarcinoma cells are more sensitive to cisplatin after a prolonged arrest in mitosis due to treatment with paclitaxel; however, no differences were found in lymph node metastases cells. We have attempted to gain insight into the molecular mechanism involved in this process, and our data has revealed that the treatment induced cell death in mitosis (MC) and apoptosis and that the strength of the G2/M checkpoint and the DNA repair pathway are responsible for the fate of the cell.

We found that after sequential PLX-CDDP treatment GC cells acquire gross nuclear alterations that constitute the most prominent morphological traits of MC. MC is a term that has been widely used to describe a form of cell death that occurs during mitosis (as reviewed in [37]). There are controversial data in the literature regarding whether apoptosis is induced during mitosis and, if so, when it is induced. Our in vivo analysis confirms that the above treatment induced cell death during mitosis, in contrast with cells treated with cisplatin alone, which die by apoptosis during the interphase. Our data also indicate that this event is partially a caspase-dependent process, because the use of pan caspase inhibitor z-VAD-fmk reduced cell death in MKN45 cells. The fact that caspase inhibitors fail to completely prevent cell death induced by treatment with spindle poisons led us to conclude that other mechanisms may play a role in mitotic cell death [37, 38]. This hypothesis agrees with recent reports showing that mitotic slippage, due to the slow but progressive cyclin B degradation in the presence of a prolonged mitotic arrest, and caspase-dependent apoptosis are mechanistically independent processes [39]. Accordingly, our present results show that cell fate after mitotic arrest seems to depend on two main factors: the sustained activity of SAC, which prevents cyclin B degradation and slippage, and the ease of triggering the apoptotic machinery. This hypothesis is supported by the fact that ST2957 cells, which showed higher levels of cyclin B during the treatment, did not activate cell death pathways. Another interesting observation is the fact that Mcl-1 is only degraded in MKN45 cells. Mitotic cell death generally occurs via intrinsic or mitochondrial apoptosis, which is regulated by the Bcl-2 family of proteins [40]. Pro-survival members, including Bcl-Xl, Bcl-2 and Mcl1, antagonize apoptosis by blocking the activity of pro-apoptotic regulators. Once Mcl-1 is phosphorylated by JNK, p38 or CKII, it is recruited to the SCF and degraded by proteasome. Mcl-1 has also been reported to be degraded by APC/C-cdc20 when it is phosphorylated by Cdk1 in mitotic arrested cells [41]. Given that we observed an increase in JNK and p38 activities during treatment, it would make sense to test whether other stimuli that activate the stress response pathway could modulate the percentage of cells that die in mitosis.

We demonstrated that sequential treatment in MKN45 cells caused the accumulation of DNA damage over time, indicating the presence of unrepaired DSBs that may lead to cell death. Two questions arise from this observation, the first of which regards the reasons paclitaxel alone induces injury to the DNA. This drug does not directly damage DNA but causes chromosome segregation errors that can increase DNA breaks [42]. The second question concerns the reasons for the lack of repair. New insights are currently emerging on how DDR is controlled during mitosis [43]. We found that BRCA1, a protein required for DNA repair by homologous recombination (HR), is not phosphorylated on the S988 residue. However, we can only hypothesize that Chk2 can phosphorylate BRCA1 on this residue (S988) to mediate the DNA damage response [44] and that this phosphorylation does occur during mitosis [45]. Accordingly, the loss of BRCA1 or impairment of its Chk2-mediated phosphorylation leads to spindle formation defects and CIN in human somatic cells [32]. Our results indicate that the event responsible for the absence of BRCA1 S988 phosphorylation could be the reduction in or the absence of Chk2 activity. The role of BRCA1 during mitosis warrants in-depth study, as does its role in repairing DNA interstrand crosslinks induced by cisplatin, as it has been reported that it plays a role independent of HR in repairing these adducts [46]. One possibility is that if the Chk2-BRCA1 pathway is deficient then there will be increased mis-attachment of spindles or an influence on the activity of the Aurora-B kinase, reducing the ability to repair merotelic attachment. Whatever the mechanism, the consequence may be increased chromosomal instability, which may be incompatible with life. The influence of BRCA1 mutations in GC after sequential PLX-CDDP treatment still needs to be clarified. In this regard, Chk2 reactivation may underlie the absence of radiological responses when bortezomib treatment was evaluated in GC patients [47]. Our data suggest that the inhibition of Chk2 may be a useful therapeutic tool in GC treatment. However, to generalize this concept, it is important to understand the cells' molecular background, given that contradictory results have been described in the literature. For example, antisense inhibition of Chk2 expression enhanced the apoptotic activity of γ-irradiation, and treatment with the topoisomerase I inhibitor camptothecin had a similar effect [48]. Furthermore, inhibition of Chk2 (with siRNA or dominant negative mutants) also enhanced adriamycin-induced apoptosis in a colon carcinoma mice model system [49]. In contrast, it has been shown that inhibition of Chk2 can lead to protection from radio- or chemotherapy [50] [51,], which may indicate that targeting Chk2 may not be beneficial for anticancer treatment. However, our findings refer to the function of Chk2 during mitosis, which has been reported as necessary for proper mitotic spindle assembly and maintenance of chromosome stability [32]. In contrast, it has been demonstrated that the loss of Chk2 promotes MC and cell death and results in suppressed oncogenic transformation and tumor development in a $Mus81^{\Delta ex3-4/\Delta ex3-4}$ background [52].

Further studies are needed to explain the contribution of p53 to cell death induced during mitosis in GC. We have shown that p53 is phosphorylated at Ser15 in GC cells in response to PXL-CDDP. There are various theories about how p53 is activated during mitosis. Our data indicate that

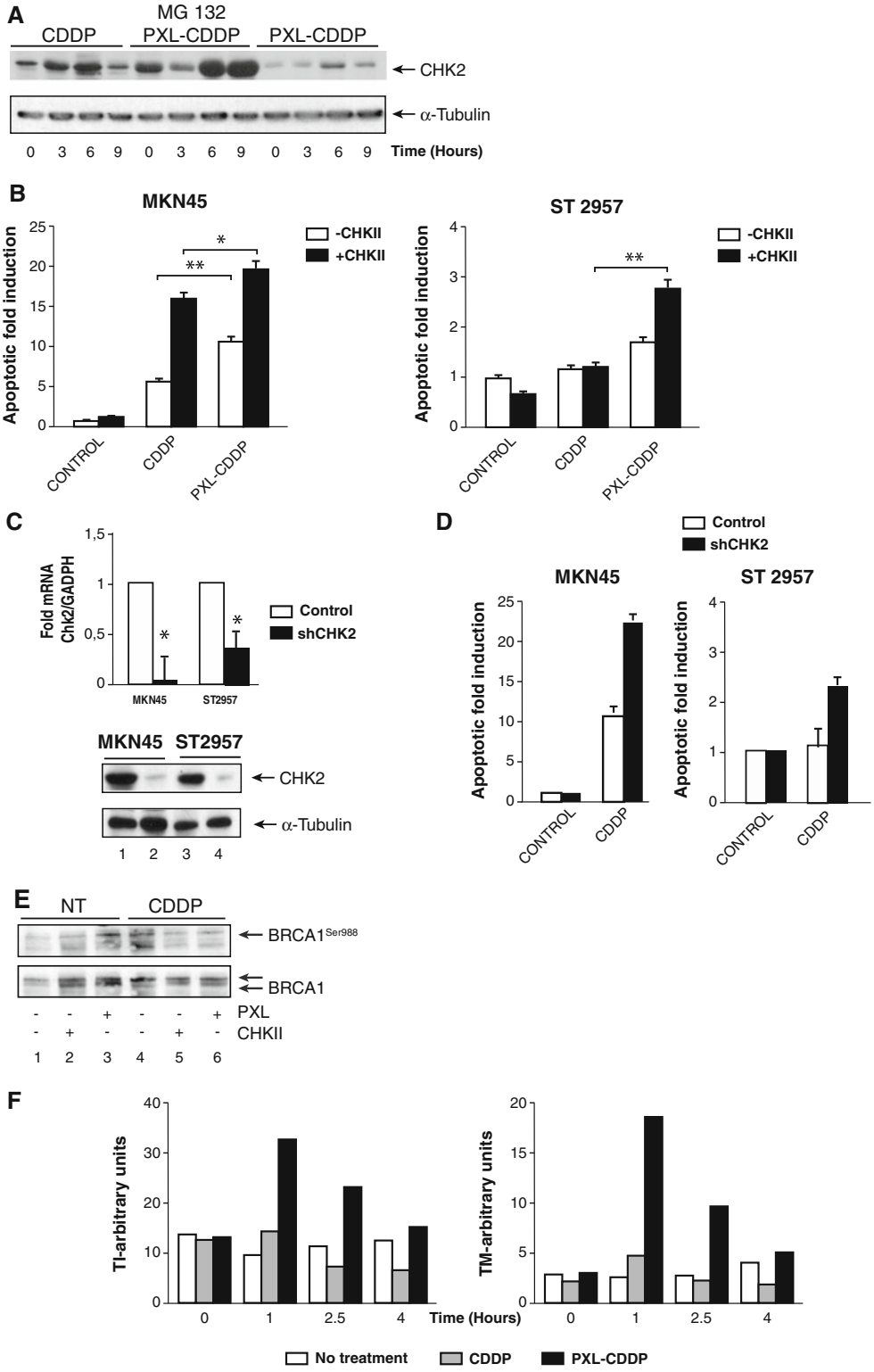

DNA damage causes activation of p53, which could be contributing to the induction of apoptosis. Along these lines, it has recently been reported that doxorubicin causes an increase in chromosome damage during anaphase in cells lacking 14-3-3σ through the activation of the γ-H2AX-path ATM-p53 pathway, which subsequently causes the cells to die [42]. Another possibility is that the cells die due to the increased transcription of pro-apoptotic members of the Bcl2

◀ **Fig. 5** Chk2 abolishment contributes to mitotic death in MKN45 cells. **a** Degradation of Chk2 is proteasome dependent. MKN45 cells were treated with PXL or PXL/CDDP in the presence or absence of the proteasome inhibitor (10 μM MG132) for 3 h, and Chk2 protein levels were detected as in Fig. 4**c**. **b** Cell cycle analyses were performed in the presence or absence of the Chk2 inhibitor (ChkII) 5 μM 1 h before CDDP addition. Cells were then treated with 10 μg/ml CDDP or PXL/CDDP (0.1 μM/10 μg/ml) for 24 h. The graph shows the percentage of apoptotic cells in each condition in the representative experiment. **c** Control and shChk2 stable cells were obtained by lentiviral infection, as described in "Materials and methods" section. Briefly, cells were transduced with lentiviral particles for control or Chk2 gene silencing and selected with 3 μg/ml puromycin. *Graph* shows the relative levels of Chk2 mRNA in the stable cells used in Fig. 5**d** after selection. Western blot is also shown to corroborate the absence of Chk2 (*bottom panel*). **d** Cells were treated with CDDP (10 μg/ml), and apoptotic cells were quantified 24 h later. **e** MKN45 cells were treated with PXL (0.1 μM), CDDP (10 μg/ml) or PXL/CDDP (0.1 μM/10 μg/ml) in the presence or absence of 5 μM ChkII (indicated with *minus* and *plus signals*) and harvested 6 h later. Extracts were probed by using specific antibodies against BRCA1^{Ser988,} and BRCA1. The *positions* of the phosphorylated BRCA1 (pBRCA1) and nonphosphorylated BRCA1 (BRCA1) are indicated. The gel lanes are indicated by *number*. The experiments were repeated twice with equivalent results. **f** The *graphs* show the DNA damage in cells not treated (*black bars*), exposed to CDDP (*grey bars*) or to the sequential treatment with PXL and CDDP (*soft grey bars*) (*left*, TM; *right*, TI) after no repair time, or 1, 2.5 and 4 h of repair. The tail moment (TM) is defined as the product of the percentage of DNA in the comet tail and the distance between the means of the tail and head fluorescence distributions. The tail intensity (TI) is defined as the percentage of DNA (fluorescent) in the tail. TM and TI are expressed in arbitrary units. Experiments were performed in duplicate. Fifty comets per duplicate gel were scored and quantified by Komet 5.5 image analysis software (Kinetic Imaging Ltd., Nottingham, UK). Apoptotic cells (non-detectable cell nuclei, ghost cells, clouds or hedgehogs) were not scored

family of proteins. Our data indicate an increase in ATM activation in response to paclitaxel, very likely a consequence of telomere dysfunction, as recently described [34].

After entering mitosis, the exit is controlled by the spindle assembly checkpoint (SAC). The SAC ensures that metaphase onset takes place when all the kinetochores are properly attached to the mitotic spindle. When bipolar conformation arises, the SAC is inactivated, and the proteolysis of cyclin B and securin allows the chromatids to separate and the cell to exit mitosis. In this study, we have shown that MKN45 cells suffer mitotic slippage, in contrast to ST2957 cells. Mitotic slippage may occur in the presence of an active SAC via cyclin B destruction. Whether bypassing the SAC correlates with cyclin B degradation in MKN45-treated cells and the influence on ST2957 cells, will be the subject of further studies. Our results suggest that GC cells treated sequentially with PLX/CDDP induce degradation of Chk2 and MC. Given that Chk2 is overexpressed in GC (50 % of cases) [53], these results suggest that combining Chk2 inhibitors with CDDP would improve therapeutic responses in this group of patients, leading to a more individualized therapy.

Acknowledgments We are grateful to Javier Perez, Daniel Gomez (photography facility), Diego Navarro and Lucia Sanchez (microscopy facility IIBM) and Diego Mejias (microscopy facility from CNIO) for technical assistance. We also would like to thank Dr. Marcos Malumbres for the GFP-H4B plasmid, R. Sanchez and Marta Fernandez-Fuente for proofreading the manuscript. This work was supported by the following Grants: PS09/1988, PI11-00949 and CCG10-UAM/BIO-5871. The authors declare no competing relationship or commercial affiliations or financial interests.

References

1. Paoletti X, Oba K, Burzykowski T et al (2010) Benefit of adjuvant chemotherapy for resectable gastric cancer: a meta-analysis. JAMA 303:1729–1737
2. Power DG, Kelsen DP, Shah MA (2010) Advanced gastric cancer–slow but steady progress. Cancer Treat Rev 36:384–392
3. Cahill R, Lindsey I, Cunningham C (2009) NOTES for colorectal neoplasia–surgery through the looking glass. Gut 58:1168–1169
4. Im CK, Jeung HC, Rha SY et al (2008) A phase II study of paclitaxel combined with infusional 5-fluorouracil and low-dose leucovorin for advanced gastric cancer. Cancer Chemother Pharmacol 61:315–321
5. Hara T, Nishikawa K, Sakatoku M, Oba K, Sakamoto J, Omura K (2011) Phase II study of weekly paclitaxel, cisplatin, and 5-fluorouracil for advanced gastric cancer. Gastric Cancer 14:332–338
6. Chua TC, Merrett ND (2012) Clinicopathologic factors associated with HER2-positive gastric cancer and its impact on survival outcomes–a systematic review. Int J Cancer 130:2845–2856
7. Yamashita-Kashima Y, Iijima S, Yorozu K et al (2011) Pertuzumab in combination with trastuzumab shows significantly enhanced antitumor activity in HER2-positive human gastric cancer xenograft models. Clin Cancer Res 17:5060–5070
8. Shiroiwa T, Fukuda T, Shimozuma K (2011) Cost-effectiveness analysis of trastuzumab to treat HER2-positive advanced gastric cancer based on the randomised ToGA trial. Br J Cancer 105:1273–1278
9. Sawaki A, Ohashi Y, Omuro Y et al (2012) Efficacy of trastuzumab in Japanese patients with HER2-positive advanced gastric or gastroesophageal junction cancer: a subgroup analysis of the Trastuzumab for gastric cancer (ToGA) study. Gastric Cancer 15:313–322
10. Wagner AD, Unverzagt S, Grothe W, et al. (2010) Chemotherapy for advanced gastric cancer. Cochrane Database Syst Rev:CD004064
11. Van Cutsem E, Moiseyenko VM, Tjulandin S et al (2006) Phase III study of docetaxel and cisplatin plus fluorouracil compared with cisplatin and fluorouracil as first-line therapy for advanced gastric cancer: a report of the V325 Study Group. J Clin Oncol 24:4991–4997
12. Jackson SP, Bartek J (2009) The DNA-damage response in human biology and disease. Nature 461:1071–1078
13. Kastan MB, Bartek J (2004) Cell-cycle checkpoints and cancer. Nature 432:316–323
14. Cha RS, Kleckner N (2002) ATR homolog Mec1 promotes fork progression, thus averting breaks in replication slow zones. Science 297:602–606
15. Ward IM, Minn K, Chen J (2004) UV-induced ataxia-telangiectasia-mutated and Rad3-related (ATR) activation requires replication stress. J Biol Chem 279:9677–9680
16. Ahn J, Urist M, Prives C (2004) The Chk2 protein kinase. DNA Repair (Amst) 3:1039–1047
17. Antoni L, Sodha N, Collins I, Garrett MD (2007) Chk2 kinase: cancer susceptibility and cancer therapy—two sides of the same coin? Nat Rev Cancer 7:925–936

18. Stracker TH, Usui T, Petrini JH (2009) Taking the time to make important decisions: the checkpoint effector kinases Chk1 and Chk2 and the DNA damage response. DNA Repair (Amst) 8: 1047–1054
19. Chen Y, Poon RY (2008) The multiple checkpoint functions of Chk1 and Chk2 in maintenance of genome stability. Front Biosci 13:5016–5029
20. van Leuken R, Clijsters L, Wolthuis R (2008) To cell cycle, swing the APC/C. Biochim Biophys Acta 1786:49–59
21. Lindqvist A, Rodriguez-Bravo V, Medema RH (2009) The decision to enter mitosis: feedback and redundancy in the mitotic entry network. J Cell Biol 185:193–202
22. Rieder CL, Maiato H (2004) Stuck in division or passing through: what happens when cells cannot satisfy the spindle assembly checkpoint. Dev Cell 7:637–651
23. Portugal J, Mansilla S, Bataller M (2010) Mechanisms of drug-induced mitotic catastrophe in cancer cells. Curr Pharm Des 16:69–78
24. Millman SE, Pagano M (2011) MCL1 meets its end during mitotic arrest. EMBO Rep 12:384–385
25. Kass EM, Jasin M (2010) Collaboration and competition between DNA double-strand break repair pathways. FEBS Lett 584: 3703–3708
26. Moynahan ME, Chiu JW, Koller BH, Jasin M (1999) Brca1 controls homology-directed DNA repair. Mol Cell 4:511–518
27. Peralta-Sastre A, Manguan-Garcia C, de Luis A et al (2010) Checkpoint kinase 1 modulates sensitivity to cisplatin after spindle checkpoint activation in SW620 cells. Int J Biochem Cell Biol 42:318–328
28. Vollmers HP, Stulle K, Dammrich J et al (1993) Characterization of four new gastric cancer cell lines. Virchows Arch B Cell Pathol Incl Mol Pathol 63:335–343
29. Sanchez-Perez I, Manguan-Garcia C, Menacho-Marquez M, Murguia JR, Perona R (2009) hCCR4/cNOT6 targets DNA-damage response proteins. Cancer Lett 273:281–291
30. Singh NP, McCoy MT, Tice RR, Schneider EL (1988) A simple technique for quantitation of low levels of DNA damage in individual cells. Exp Cell Res 175:184–191
31. Stolz A, Ertych N, Kienitz A et al (2010) The Chk2-BRCA1 tumour suppressor pathway ensures chromosomal stability in human somatic cells. Nat Cell Biol 12:492–499
32. Stolz A, Ertych N, Bastians H (2011) Tumor suppressor Chk2: regulator of DNA damage response and mediator of chromosomal stability. Clin Cancer Res 17:401–405
33. Sato K, Ohta T, Venkitaraman AR (2010) A mitotic role for the DNA damage-responsive Chk2 kinase. Nat Cell Biol 12:424–425
34. Hayashi MT, Cesare AJ, Fitzpatrick JA, Lazzerini-Denchi E, Karlseder J (2012) A telomere-dependent DNA damage checkpoint induced by prolonged mitotic arrest. Nat Struct Mol Biol 19:387–394
35. Branham MT, Nadin SB, Vargas-Roig LM, Ciocca DR (2004) DNA damage induced by paclitaxel and DNA repair capability of peripheral blood lymphocytes as evaluated by the alkaline comet assay. Mutat Res 560:11–17
36. Sun RG, Chen WF, Qi H et al (2012) Biologic effects of SMF and paclitaxel on K562 human leukemia cells. Gen Physiol Biophys 31:1–10
37. Vitale I, Galluzzi L, Castedo M, Kroemer G (2011) Mitotic catastrophe: a mechanism for avoiding genomic instability. Nat Rev Mol Cell Biol 12:385–392
38. Huang HC, Shi J, Orth JD, Mitchison TJ (2009) Evidence that mitotic exit is a better cancer therapeutic target than spindle assembly. Cancer Cell 16:347–358
39. Huang HC, Mitchison TJ, Shi J (2010) Stochastic competition between mechanistically independent slippage and death pathways determines cell fate during mitotic arrest. PLoS ONE 5:e15724
40. Letai AG (2008) Diagnosing and exploiting cancer's addiction to blocks in apoptosis. Nat Rev Cancer 8:121–132
41. Harley ME, Allan LA, Sanderson HS, Clarke PR (2010) Phosphorylation of Mcl-1 by CDK1-cyclin B1 initiates its Cdc20-dependent destruction during mitotic arrest. EMBO J 29:2407–2420
42. Crasta K, Ganem NJ, Dagher R et al (2012) DNA breaks and chromosome pulverization from errors in mitosis. Nature 482: 53–58
43. Yu B, Dalton WB, Yang VW (2012) CDK1 regulates mediator of DNA damage checkpoint 1 during mitotic DNA damage. Cancer Res 72:5448–5453
44. Okada S, Ouchi T (2003) Cell cycle differences in DNA damage-induced BRCA1 phosphorylation affect its subcellular localization. J Biol Chem 278:2015–2020
45. Zhang J, Willers H, Feng Z et al (2004) Chk2 phosphorylation of BRCA1 regulates DNA double-strand break repair. Mol Cell Biol 24:708–718
46. Bunting SF, Callen E, Kozak ML et al (2012) BRCA1 functions independently of homologous recombination in DNA interstrand crosslink repair. Mol Cell 46:125–135
47. Shah MA, Power DG, Kindler HL et al (2011) A multicenter, phase II study of Bortezomib (PS-341) in patients with unresectable or metastatic gastric and gastroesophageal junction adenocarcinoma. Invest New Drugs 29:1475–1481
48. Yu Q, Rose JH, Zhang H, Pommier Y (2001) Antisense inhibition of Chk2/hCds1 expression attenuates DNA damage-induced S and G2 checkpoints and enhances apoptotic activity in HEK-293 cells. FEBS Lett 505:7–12
49. Ghosh JC, Dohi T, Raskett CM, Kowalik TF, Altieri DC (2006) Activated checkpoint kinase 2 provides a survival signal for tumor cells. Cancer Res 66:11576–11579
50. Carlessi L, Buscemi G, Larson G, Hong Z, Wu JZ, Delia D (2007) Biochemical and cellular characterization of VRX0466617, a novel and selective inhibitor for the checkpoint kinase Chk2. Mol Cancer Ther 6:935–944
51. Pires IM, Ward TH, Dive C (2010) Oxaliplatin responses in colorectal cancer cells are modulated by Chk2 kinase inhibitors. Br J Pharmacol 159:1326–1338
52. El Ghamrasni S, Pamidi A, Halaby MJ et al (2011) Inactivation of Chk2 and mus81 leads to impaired lymphocytes development, reduced genomic instability, and suppression of cancer. PLoS Genet 7:e1001385
53. Shigeishi H, Yokozaki H, Oue N et al (2002) Increased expression of Chk2 in human gastric carcinomas harboring p53 mutations. Int J Cancer 99:58–62